Optical pumping via incoherent Raman transitions

A. D. Boozer, R. Miller, T. E. Northup, A. Boca, and H. J. Kimble

Norman Bridge Laboratory of Physics 12-33, California Institute of Technology, Pasadena, California 91125, USA
(Received 2 October 2007; published 3 December 2007)

An optical pumping scheme is presented that uses incoherent Raman transitions to prepare a trapped cesium atom in a specific Zeeman state within the $6S_{1/2}$, $F=3$ hyperfine manifold. An important advantage of this scheme over existing optical pumping schemes is that the atom can be prepared in any of the $F=3$ Zeeman states. We describe an experimental implementation of the scheme and show that a fraction 0.57 ± 0.02 of the total population can be prepared in the desired state, with the remaining population distributed fairly uniformly among the six other states. We demonstrate the scheme in the context of cavity quantum electrodynamics, but the technique is equally applicable to a wide variety of atomic systems with hyperfine ground-state structure.

I. INTRODUCTION

Many experiments in atomic physics rely on the ability to prepare atoms in specific internal states. For example, spin-polarized alkali-metal atoms can be used to polarize the nuclei of noble gases [1], to act as sensitive magnetometers [2], and to provide frequency standards that exploit magnetic-field-insensitive clock transitions [3]. In the field of quantum information science, internal atomic states can be used to store and process quantum bits [4–8] with extended coherence times.

A standard method for preparing an atom in a specific internal state is optical pumping [9–11], which involves driving the atom with light fields that couple to all but one of its internal states; these light fields randomly scatter the atom from one internal state to another until it falls into the uncoupled "dark" state. Various optical pumping schemes have been analyzed and demonstrated for alkali-metal atoms [3,12,13] and today are well-established techniques. These schemes rely on dark states that are set by the polarization of the driving field, and this imposes restrictions on the possible Zeeman states in which the atom can be prepared. Specifically, one can prepare the atom in the $m_F=0$ state by using light that is linearly polarized along the quantization axis, or in one of the edge states ($m_F=\pm F$) by using light that is circularly $\sigma_{\pm}$ polarized along the quantization axis.

In contrast, the scheme presented here allows the atom to be prepared in any of the Zeeman states within the lowest ground-state hyperfine manifold of an alkali-metal atom, which in our case is the $6S_{1/2}$, $F=3$ manifold of cesium. The key component of the scheme is a pair of optical fields that drive Raman transitions between pairs of Zeeman states $|3,m\rangle \leftrightarrow |4,m\rangle$. We apply a magnetic bias field to split out the individual Zeeman transitions, and add broadband noise to one of the optical fields, where the spectrum of the noise is tailored such that all but one of the transitions are driven. The two Zeeman states corresponding to the undriven transition are the dark states of the system, and we exploit these dark states to perform optical pumping. We verify the optical pumping by using coherent Raman transitions to map out a Raman spectrum, which allows us to determine how the atomic population is distributed among the different Zeeman states; these measurements show that a fraction 0.57±0.02 of

the total population is prepared in the desired state, with the remaining population distributed fairly uniformly among the six other states. The capability of driving Raman transitions between hyperfine ground states has many additional applications, such as state manipulation [14], ground-state cooling [15–18], precision measurements [19,20], and Raman spectroscopy [21]. The scheme described here shows that this versatile tool can also be used for atomic state preparation.

We have demonstrated this scheme in the context of cavity quantum electrodynamics (QED), specifically in a system in which a single atom is strongly coupled to a high-finesse optical cavity. Cavity QED offers a powerful resource for quantum information science, and the ability to prepare the atom in a well-defined initial state is a key requirement for many of the protocols that have been proposed for this system, such as the generation of polarized single photons [22,23] and the transfer of Zeeman coherence to photons within the cavity mode [24]. Conventional optical pumping to a single Zeeman sublevel has been previously demonstrated within a cavity [25], but we find our method to be particularly effective given the constraints of our system, in which optical access to the atom is limited and we must address the large multiplicity of cesium sublevels. However, optical pumping via incoherent Raman transitions has much broader applications beyond the cavity QED setting, and can be used in a wide variety of atomic systems with hyperfine ground-state structure.

II. EXPERIMENTAL APPARATUS

Our system consists of a single cesium atom that is strongly coupled to a high-finesse optical cavity, as shown in Fig. 1. The cavity supports a set of discrete modes, and its length is tuned so that one pair of modes [26] is nearly resonant with the atomic transition $6S_{1/2}$, $F=4 \rightarrow 6P_{3/2}$, $F=5'$ at $\lambda_{D2}=852$ nm (see the level diagram shown in Fig. 2). The atomic dipole associated with this transition couples to the electric field of the resonant mode, allowing the atom and cavity to exchange excitation at a characteristic rate $g = (2\pi)(34$ MHz$)$ for the $6S_{1/2}$, $F=4$, $m_F=4 \rightarrow 6P_{3/2}$, $F=5'$, $m_{F'}=5$ transition, a rate that is much larger than either the cavity decay rate $\kappa=(2\pi)(3.8$ MHz$)$ or the atomic decay rate
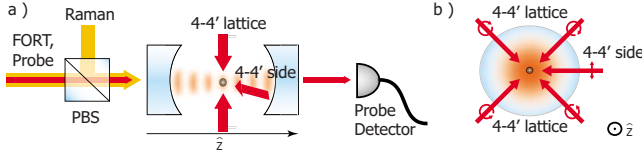
FIG. 1. (Color online) Schematic of experiment. (a) View from the side of the cavity. Shown are the linearly polarized FORT, Raman, and probe beams that drive the cavity, and the circularly polarized 4-4′ lattice beams and linearly polarized 4-4′ side beam that drive the atom. (b) View along the cavity axis. Shown are the 4-4′ lattice beams and the 4-4′ side beam.

$\gamma=(2\pi)(2.6 \text{ MHz})$; thus, the system is in the strong-coupling regime [27].

We hold the atom inside the cavity via a state-insensitive far off-resonance trap (FORT) [28]. The FORT is produced by resonantly driving a cavity mode at $\lambda_F=936$ nm with a linearly polarized beam, which creates a red-detuned standing wave inside the cavity. Each antinode of this standing wave forms a potential well in which an atom can be trapped; for the experiments described here, the optical power of the FORT beam is chosen such that the depth of these wells is $U_F=(2\pi)(45 \text{ MHz})$.

We drive Raman transitions between the $F=3$ and $F=4$ hyperfine ground-state manifolds of the atom by adding a second beam, referred to here as the Raman beam, which drives the same cavity mode as the FORT beam but is detuned from the FORT by the atomic hyperfine splitting $\Delta_{\text{HF}}=(2\pi)(9.2 \text{ GHz})$ (this scheme was first proposed in [29], and was used to perform Raman sideband cooling in [30]). The FORT and Raman beams are combined on a polarizing beam splitter (PBS) before entering the cavity, so the Raman beam is linearly polarized in a direction orthogonal to the polarization of the FORT beam. To stabilize the frequency difference between the FORT and Raman beams, the external-cavity diode laser that generates the Raman beam is injection locked to the red sideband of light that has been picked off from the FORT beam and passed through an electro-optical modulator (EOM), which is driven at Δ_{HF}. The FORT and Raman beams form the two legs of a Raman pair and drive Raman transitions between pairs of Zeeman states $|3,m\rangle \leftrightarrow |4,m\rangle$, where the quantization axis $\hat{z}$ is chosen to lie
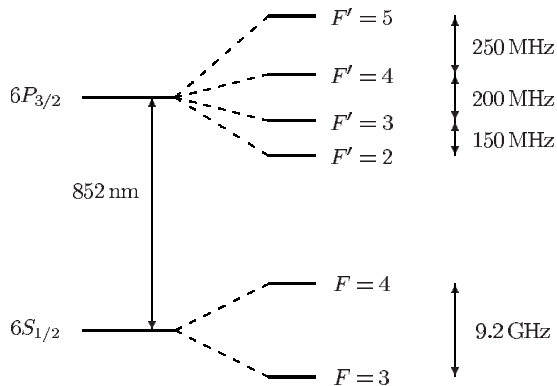

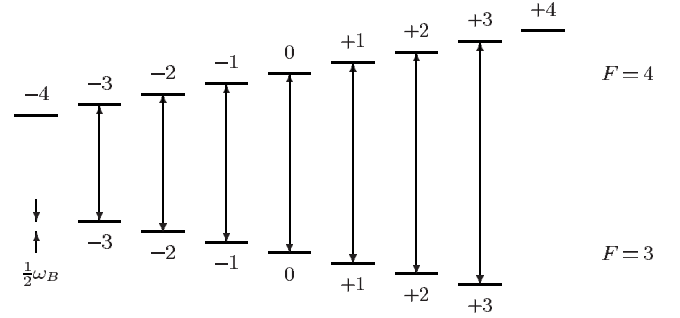FIG. 2. Level diagram for the $D2$ line in cesium.

FIG. 3. Ground-state spectrum of cesium in the presence of an axial bias field. The Raman coupling drives transitions between pairs of Zeeman states $|3,m\rangle \leftrightarrow |4,m\rangle$, as indicated by the arrows.

along the cavity axis [31]. Typically we use a strong FORT beam and a weak Raman beam, so the Raman beam does not significantly alter the FORT trapping potential [32].

In order to address individual Zeeman transitions, we apply a magnetic bias field B_a along the cavity axis. As shown in Fig. 3, this axial field shifts the $|3,m\rangle \leftrightarrow |4,m\rangle$ transition by

$$\delta(|3,m\rangle \leftrightarrow |4,m\rangle) = \omega_B m, \quad (1)$$

where

$$\omega_B \equiv (g_4 - g_3)\mu_B B_a = (2\pi)(700 \text{ kHz/G})B_a, \quad (2)$$

and $g_4=1/4$, $g_3=-1/4$ are the Lande g factors for the $F=4$ and $F=3$ ground-state hyperfine manifolds. For the experiments described here, we typically set the axial bias field such that $\omega_B \simeq (2\pi)(910 \text{ kHz})$.

The strong atom-cavity coupling allows us to determine whether the atom is in the $F=3$ or $F=4$ hyperfine manifold by driving the cavity with a 100 μs pulse of resonant 4-5′ probe light, as described in [18]. If the atom is in $F=4$, it couples to the cavity and blocks the transmission of the probe beam, while if the atom is in $F=3$, it decouples from the cavity, and the probe beam is transmitted. Using this technique, we can determine the hyperfine ground state of the atom with an accuracy of ~98% for a single 100 μs measurement interval.

Atoms are delivered to the cavity by releasing a magneto-optical trap located a few millimeters above the cavity, and the falling atoms are loaded into the FORT by cooling them with 4-4′ lattice light. This lattice light consists of two pairs of counterpropagating beams in the $\sigma_+ - \sigma_-$ configuration, which are applied from the sides of the cavity. We ensure that only one atom is trapped in the FORT by applying the Raman beam and driving the cavity with a resonant 4-5′ probe; this combination gives an effect analogous to that in [33], which allows us to determine the number of atoms in the cavity based on the amount of 4-5′ light that is transmitted.

III. COHERENT AND INCOHERENT RAMAN TRANSITIONS

If the FORT and Raman beams are both monochromatic, then they drive coherent Raman transitions between pairs of

Zeeman states $|3,m\rangle \leftrightarrow |4,m\rangle$, and the atomic populations oscillate between the two states in each pair. The effective Rabi frequency for the $|3,m\rangle \leftrightarrow |4,m\rangle$ transition is

$$\Omega_E(|3,m\rangle \leftrightarrow |4,m\rangle) = \Omega_0(1 - m^2/16)^{1/2}, \qquad (3)$$

where Ω_0 is set by the power in the FORT and Raman beams [29]. For the experiments described here, the powers in these beams are chosen such that $\Omega_0 \simeq (2\pi)(120 \text{ kHz})$. The Raman detuning for the FORT-Raman pair is given by $\delta_R = \omega_F - \omega_R - \Delta_{HF}$, where ω_F and ω_R are the optical frequencies of the FORT and Raman beams, which means that the effective detuning for the $|3,m\rangle \leftrightarrow |4,m\rangle$ transition is

$$\delta_E(|3,m\rangle \leftrightarrow |4,m\rangle) = \delta_R - \omega_B m. \qquad (4)$$

We can also drive incoherent Raman transitions by using a monochromatic FORT beam and a spectrally broad Raman beam, where the spectral width is typically ~ 10 MHz. In contrast to coherent Raman transitions, in which the atom undergoes coherent Rabi oscillations, for incoherent Raman transitions the atomic population decays at a constant rate from $|3,m\rangle \rightarrow |4,m\rangle$ and from $|4,m\rangle \rightarrow |3,m\rangle$. In the Appendix, we show that these decay rates are proportional to $S(\Delta_{HF} + \omega_B m)$, where $S(\omega)$ is the power spectrum of a beat note formed between the FORT and Raman beams.

IV. MEASURING THE POPULATION DISTRIBUTION

Given an initial state of the atom in which the entire population lies in the $F=3$ manifold, we can use coherent Raman transitions to determine how the population is distributed among the various Zeeman states. To perform this measurement we prepare the atom in the desired initial state, apply a coherent Raman pulse of fixed duration, Rabi frequency, and Raman detuning, and then drive the cavity with a resonant $F=4 \rightarrow F=5'$ probe beam to determine if the atom was transferred to $F=4$. By iterating this process we determine the probability p_4 for the atom to be transferred by the Raman pulse, and by repeating the probability measurement for different Raman detunings δ_R we can map out a Raman spectrum $p_4(\delta_R)$. For the Raman spectra presented here, the Raman pulses have Rabi frequency $\Omega_0 = (2\pi)(120 \text{ kHz})$ and duration 25 μs. This is long enough that the Rabi oscillations decohere, and the Raman spectrum just records the Lorentzian envelope for each Zeeman transition. Thus, when the $|3,m\rangle \leftrightarrow |4,m\rangle$ Zeeman transition is resonantly driven by the Raman pulse, roughly one-half of the population that was initially in $|3,m\rangle$ is transferred to $|4,m\rangle$.

As a demonstration of this technique, Fig. 4 shows a Raman spectrum for an initial state with comparable populations in all of the $F=3$ Zeeman states. To prepare this state, we optically pump the atom to $F=3$ by alternating seven pulses of resonant $F=4 \rightarrow F=4'$ lattice light with seven pulses of resonant $F=4 \rightarrow F=4'$ side light, where each pulse is 300 ns long. The beams that deliver the lattice and side light are shown in Fig. 1.

To determine the population $p_{3,m}$ in the Zeeman state $|3,m\rangle$, we fit a sum of Lorentzians, one for each Zeeman transition, to the experimental data,
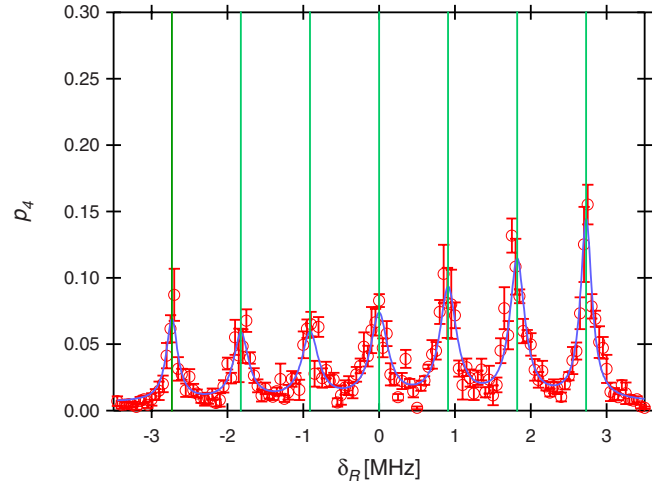

FIG. 4. (Color online) Raman spectrum for a random initial state. Shown is the transfer probability p_4 versus Raman detuning δ_R: the points are the experimental data, the curve is a fit of $p_4(\delta_R)$, as given by Eq. (5), and the vertical green lines indicate the predicted frequencies $\delta(|3,m\rangle \leftrightarrow |4,m\rangle)$ for individual Zeeman transitions.

$$p_4(\delta_R) = p_b + (1/2)$$
$$\times \sum_m [1 + (\delta_R - \omega_B m)^2/(1 - m^2/16)\Omega_0^2]^{-1} p_{3,m}, \qquad (5)$$

where p_b is a constant background. We fit the Zeeman state populations, the Rabi frequency Ω_0, and the frequency ω_B that characterizes the strength of the axial bias field, and perform an independent measurement to determine the background probability $p_b = 0.006$. The fitted value of Ω_0 agrees to within 14% with the value we would expect based on the measured optical powers in the FORT and Raman beams, and the fitted value of ω_B agrees to within 5% with the value we would expect based on the known axial coil current and geometry. As a consistency check we sum the fitted populations and obtain the result 1.10 ± 0.03, in reasonable agreement with the expected value of 1.

V. OPTICAL PUMPING SCHEME

We can prepare the atom in a specific Zeeman state by using a Raman beam whose spectrum is tailored to incoherently drive all but one of the Zeeman transitions. As an example, Fig. 5(a) shows the power spectrum of the noise used for pumping into $|3,0\rangle$. This graph was obtained by measuring the power spectrum of a beat note formed between the FORT and Raman beams by mixing them on a photodetector with a nonpolarizing beam splitter. For comparison, Fig. 5(b) shows the power spectrum for a monochromatic Raman beam tuned to Raman resonance, as would be used for driving coherent Raman transitions.

Comparing the noise spectrum shown in Fig. 5(a) to the Raman spectrum shown in Fig. 4, we see that the noise drives incoherent Raman transitions from $|3,m\rangle \leftrightarrow |4,m\rangle$ for $m \neq 0$, but because of the notch around zero detuning, the $|3,0\rangle \leftrightarrow |4,0\rangle$ transition is not driven. We optically pump the
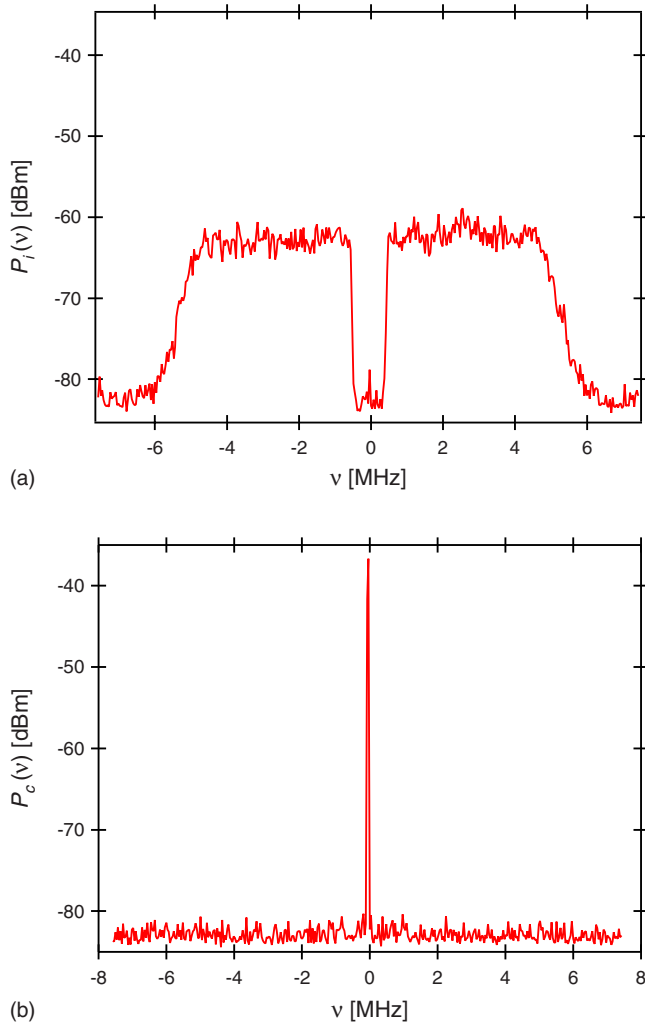
FIG. 5. (Color online) (a) Power spectrum of noise used for pumping into $|3,0\rangle$. (b) Power spectrum of coherent signal used for driving coherent Raman transitions with $\Omega_0 = (2\pi)(120 \text{ kHz})$. Both curves are obtained by combining the FORT and Raman beams on a photodetector and measuring the spectrum of the photocurrent; shown is the rf power in a 3 kHz bandwidth versus detuning from Δ_{HF}.

FIG. 6. (Color online) (a) Raman spectrum for optical pumping into $|3,0\rangle$. (b) Raman spectrum for optical pumping into $|3,1\rangle$. Raman spectrum for a random initial state. Shown is the transfer probability p_4 versus Raman detuning δ_R: the points are the experimental data, the curve is a fit of $p_4(\delta_R)$, as given by Eq. (5), and the vertical green lines indicate the predicted frequencies $\delta(|3,m\rangle \leftrightarrow |4,m\rangle)$ for individual Zeeman transitions.

atom into $|3,0\rangle$ by first driving incoherent Raman transitions for 10 μs, then pumping the atom to $F=3$ using the method discussed in Sec. IV, and iterating this sequence 40 times. It is straightforward to modify this procedure so as to pump into the $|3,m\rangle$ Zeeman state for any m; we simply shift the notch in the noise so that it overlaps with the $|3,m\rangle \leftrightarrow |4,m\rangle$ transition.

To characterize the optical pumping, we first pump the atom into a specific Zeeman state and then measure the Raman spectrum as described in the preceding section. Figure 6 shows Raman spectra measured after pumping into (a) $|3,0\rangle$ and (b) $|3,1\rangle$. We find that the fraction of the atomic population in the desired state is 0.57 ± 0.02 for pumping into $|3,0\rangle$ and 0.57 ± 0.02 for pumping into $|3,1\rangle$, where the remaining population is roughly equally distributed among the other Zeeman states [these numbers are obtained by fitting Eq. (5) to the data, as described in Sec. IV]. Summing the
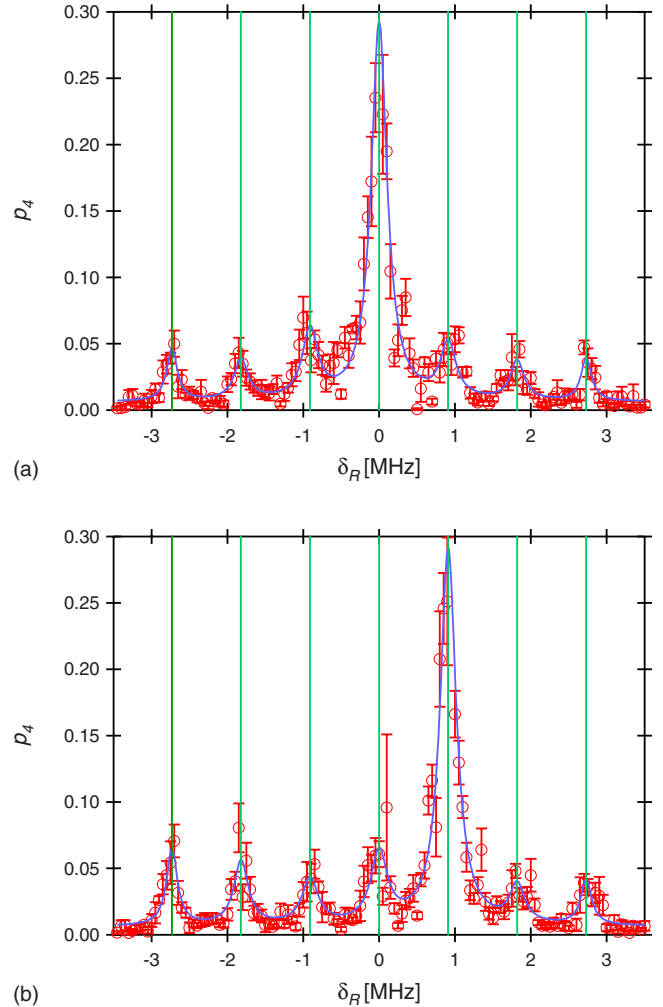
fitted populations in all the Zeeman states, we obtain the value 1.02 ± 0.04 for (a) and 1.08 ± 0.04 for (b), in reasonable agreement with the expected value of 1.

To generate the Raman beam used in Fig. 5(a), we start with an rf noise source, which produces broadband noise that is spectrally flat from dc to ~ 10 MHz. The noise is passed through a high-pass filter at 500 kHz and a low-pass filter at 5 MHz, where both filters roll off at 60 dB per octave. The filtered noise is then mixed against an 85 MHz local oscillator, and the resulting rf signal is used to drive an acousto-optical modulator (AOM) that modulates a coherent beam from the injection-locked Raman laser. The first order diffracted beam from the AOM forms a Raman beam with the desired optical spectrum. Note that previous work has demonstrated the use of both synthesized incoherent laser fields [34,35], such as that used here, as well as the noise intrinsic to free-running diode lasers [36,37] to resonantly probe atomic spectra.

Although the scheme presented here relies on incoherent Raman transitions, it is also possible to perform optical pumping with coherent Raman transitions. The basic principle is the same: we simultaneously drive all but one of the Zeeman transitions, only instead of using a spectrally broad Raman beam, we use six monochromatic Raman beams, where each beam is tuned so as to resonantly drive a different transition. We have implemented such a scheme, and found that it gives comparable results to the incoherent scheme described above, but there are two advantages to the incoherent scheme. First, it is simpler to generate a Raman beam with the necessary spectral properties for the incoherent scheme. Second, when coherent Raman transitions are used, the six frequency components for the Raman beam must be tuned to resonance with their respective transitions, and hence are sensitive to the value of the axial magnetic field. When incoherent Raman transitions are used, however, the same Raman beam can be used for a broad range of axial field values.

VI. CONCLUSION

We have proposed a scheme for optically pumping atoms into a specific Zeeman state and have experimentally implemented the scheme with cesium atoms in a cavity QED setting. An important advantage over existing schemes is that atoms can be prepared in any of the Zeeman states in the lower hyperfine ground-state manifold.

We have measured the effectiveness of the optical pumping, and have shown that a fraction ~ 0.57 of the atomic population can be prepared in the desired Zeeman state. Some possible factors that could be limiting the effectiveness of the optical pumping include fluctuating magnetic fields transverse to the cavity axis, misalignment of the cavity axis with the axial bias field, and slow leaking out of the dark state due to scattering from background light. We are currently investigating these factors.

The scheme presented here operates on a fundamentally different principle from existing optical pumping schemes, in that it relies on incoherent Raman transitions to create an atomic dark state. Raman transitions have many different applications in atomic physics, so there are often independent reasons for incorporating a system for driving Raman transitions into an atomic physics laboratory; our scheme shows that such a system can also be applied to the problem of atomic state preparation. The scheme should serve as a useful tool for experiments in atomic physics, both in a cavity QED setting and beyond.

APPENDIX: TRANSITION RATE FOR INCOHERENT RAMAN TRANSITIONS

As described in Sec. III, we drive incoherent Raman transitions between pairs of Zeeman states $|3,m\rangle \leftrightarrow |4,m\rangle$ by us-

ing a monochromatic FORT beam and a spectrally broad Raman beam. For incoherent Raman transitions the atomic population decays at a constant rate from $|3,m\rangle \rightarrow |4,m\rangle$ and from $|4,m\rangle \rightarrow |3,m\rangle$, and in this appendix we calculate these decay rates.

We will consider a single Zeeman transition $|3,m\rangle \leftrightarrow |4,m\rangle$, so we can treat the system as an effective two-level atom with ground state $g \equiv |3,m\rangle$ and excited state $e \equiv |4,m\rangle$, where the energy splitting between g and e is $\omega_A \equiv \Delta_{HF} + \omega_B m$. The FORT-Raman pair drives this effective two-level atom with broadband noise, which we can approximate as a comb of classical fields with optical frequencies ω_k and Rabi frequencies Ω_k. Let us assume that we start in the ground state g. If we only consider the coupling of the atom to field k, then the equation of motion for the excited state amplitude c_e is

$$i\dot{c}_e = \frac{\Omega_k}{2} e^{-i\delta_k t} c_g, \tag{A1}$$

where $\delta_k \equiv \omega_k - \omega_A$ is the detuning of the field from the atom. At small times the population is almost entirely in the ground state, so we can make the approximation $c_g = 1$ and integrate Eq. (A1) to obtain

$$c_e(t) = \frac{\Omega_k}{2\delta_k} (e^{-i\delta_k t} - 1). \tag{A2}$$

Thus, the transition rate from g to e for a single frequency ω_k is

$$\gamma_k = \frac{|c_e(t)|^2}{t} = \frac{\pi}{4} t \Omega_k^2 D(\delta_k t/2), \tag{A3}$$

where

$$D(x) \equiv \frac{\sin^2 x}{\pi x^2}. \tag{A4}$$

The total decay rate is obtained by summing the decay rates for all the fields in the comb,

$$\gamma = \sum_k \gamma_k = \frac{\pi}{4} t \sum_k \Omega_k^2 D(\delta_k t/2). \tag{A5}$$

To evaluate this expression we need to know the distribution of Rabi frequencies Ω_k. This information can be obtained by forming a beat note between the FORT and Raman beams on a photodetector, and measuring the power spectrum $S(\omega)$ of the photocurrent using a spectrum analyzer. Let us first consider this measurement for a monochromatic Raman beam, and then generalize to a spectrally broad Raman beam. If both the FORT and Raman beams are monochromatic, with optical frequencies ω_F and ω_R, then the resulting photocurrent $i(t)$ is given by

$$i(t) = i_F + i_R + 2\eta \cos[(\omega_F - \omega_R)t] \sqrt{i_F i_R}, \tag{A6}$$

where i_F and i_R are the cycle-averaged photocurrents for the FORT and Raman beams taken individually and η is the heterodyne efficiency. Thus, the power spectrum of the photocurrent has a spike at the difference frequency $\Delta \equiv \omega_F - \omega_R$,

$$S_c(\omega) = P_c\delta(\omega - \Delta), \qquad (A7)$$

where the integrated power P_c of the spike is proportional to $i_F i_R$. If the difference frequency Δ is tuned to Raman resonance ($\Delta = \omega_A$), then the FORT-Raman pair drives coherent Raman transitions with a Rabi frequency Ω_c that is proportional to $\sqrt{i_F i_R}$, so

$$\Omega_c^2 = \alpha P_c, \qquad (A8)$$

where α is a constant that depends on various calibration factors.

Now consider the case of a spectrally broad Raman beam, which results in a photocurrent with power spectrum $S_i(\omega)$. The effective Rabi frequency Ω_k corresponding to comb line k is given by

$$\Omega_k^2 = \alpha S_i(\omega_k)\delta\omega, \qquad (A9)$$

where $\delta\omega$ is the frequency spacing between adjacent comb lines. Substituting this result into Eq. (A5), and replacing the sum with an integral, we obtain

$$\gamma = \frac{\pi}{4}\alpha t \int S_i(\omega)D[(\omega - \omega_A)t/2]d\omega. \qquad (A10)$$

If the power spectrum near ω_A is flat over a bandwidth $\sim 1/t$, then we can approximate D as a δ function and perform the integral

$$\gamma = \frac{\pi}{2}\alpha S_i(\omega_A). \qquad (A11)$$

It is convenient to use Eq. (A8) to eliminate the calibration factor α,

$$\gamma = \frac{\pi}{2}\frac{S_i(\omega_A)}{P_c}\Omega_c^2. \qquad (A12)$$

The spectrum analyzer trace given in Fig. 5(a) displays the power spectrum in terms of the power $P_i(\nu) \simeq 2\pi B S_i(\omega)$ in a

bandwidth $B = 3$ kHz, so we can also write this as

$$\gamma = \frac{1}{4}\frac{P_i(\omega_A/2\pi)}{P_c}\frac{\Omega_c^2}{B} = \frac{1}{4}(1 - m^2/16)\frac{\Omega_0^2}{B}\frac{P_i[(\Delta_{\rm HF} + \omega_B m)/2\pi]}{P_c}, \qquad (A13)$$

where we have substituted $\Omega_c = (1 - m^2/16)^{1/2}\Omega_0$ and $\omega_A = \Delta_{\rm HF} + \omega_B m$.

We can calculate the time evolution of the atomic populations using rate equations. It is straightforward to show that the decay rate $e \to g$ is also given by γ, and from the rate equations one can show that the excited state population is

$$p_e(t) = \frac{1}{2}[1 - \exp(-2\gamma t)]. \qquad (A14)$$

We can calculate the decay rates for the noise spectrum shown in Fig. 5. For this noise spectrum the power $P_i(\nu)$ has roughly the same value $\bar{P}_i$ at the frequencies of all the $m \neq 0$ Zeeman transitions, so we can write the decay rates for these transitions as

$$\gamma(|3,m\rangle \to |4,m\rangle) = \gamma(|4,m\rangle \to |3,m\rangle) = (1 - m^2/16)\Gamma, \qquad (A15)$$

where

$$\Gamma \equiv (1/4)(\Omega_0^2/B)(\bar{P}_i/P_c). \qquad (A16)$$

From the power spectrum for the noise shown in Fig. 5(a) we have that $\bar{P}_i = -63$ dBm, and from the power spectrum for the coherent signal shown in Fig. 5(b) we have that $P_c = -36$ dBm, where the corresponding Rabi frequency is $\Omega_0 = (2\pi)(120$ kHz). Substituting these values into Eq. (A16), we obtain $\Gamma = 0.084$ μs^{-1}.

[1] T. G. Walker and W. Happer, Rev. Mod. Phys. **69**, 629 (1997).
[2] D. Budker, W. Gawlik, D. F. Kimball, S. M. Rochester, V. V. Yashchuk, and A. Weis, Rev. Mod. Phys. **74**, 1153 (2002).
[3] C. Audoin, Metrologia **29**, 113 (1992).
[4] J. I. Cirac, P. Zoller, H. J. Kimble, and H. Mabuchi, Phys. Rev. Lett. **78**, 3221 (1997).
[5] P. Zoller *et al.*, Eur. Phys. J. D **36**, 203 (2005).
[6] J. Laurat, K. S. Choi, H. Deng, C. W. Chou, and H. J. Kimble, Phys. Rev. Lett. **99**, 180504 (2007).
[7] C. W. Chou, J. Laurat, H. Deng, K. S. Choi, H. de Riedmatten, D. Felinto, and H. J. Kimble, Science **316**, 1316 (2007).
[8] D. Leibfried, R. Blatt, C. Monroe, and D. Wineland, Rev. Mod. Phys. **75**, 281 (2003).
[9] A. Kastler, Nobel Prize Lecture, 1966.
[10] W. Demtroder, *Laser Spectroscopy: Basic Concepts and Instrumentation* (Springer-Verlag, Berlin, 1982), p. 567.
[11] W. Happer, Rev. Mod. Phys. **44**, 169 (1972).
[12] L. S. Cutler, U.S. Patent No. 4,425,653 (1984).
[13] B. Wang, Y. Han, J. Xiao, X. Yang, C. Zhang, H. Wang, M. Xiao, and K. Peng, Phys. Rev. A **75**, 051801(R) (2007).
[14] D. J. Wineland, M. Barrett, J. Britton, J. Chiaverini, B. L. DeMarco, W. M. Itano, B. M. Jelenkovic, C. Langer, D. Leibfried, V. Meyer, T. Rosenband, and T. Schaetz, Philos. Trans. R. Soc. London, Ser. A **361**, 1349 (2003).
[15] C. Monroe, D. M. Meekhof, B. E. King, S. R. Jefferts, W. M. Itano, D. J. Wineland, and P. Gould, Phys. Rev. Lett. **75**, 4011 (1995).
[16] S. E. Hamann, D. L. Haycock, G. Klose, P. H. Pax, I. H. Deutsch, and P. S. Jessen, Phys. Rev. Lett. **80**, 4149 (1998).
[17] V. Vuletic, C. Chin, A. J. Kerman, and S. Chu, Phys. Rev. Lett. **81**, 5768 (1998).
[18] A. D. Boozer, A. Boca, R. Miller, T. E. Northup, and H. J. Kimble, Phys. Rev. Lett. **97**, 083602 (2006).
[19] P. Clade, E. de Mirandes, M. Cadoret, S. Guellati-Khelifa, C.

Schwob, F. Nez, L. Julien, and F. Biraben, Phys. Rev. Lett. **96**, 033001 (2006).

[20] T. L. Gustavson, P. Bouyer, and M. A. Kasevich, Phys. Rev. Lett. **78**, 2046 (1997).

[21] I. Dotsenko, W. Alot, S. Kuhr, D. Schrader, M. Muller, Y. Miroshnychenko, V. Gomer, A. Rauschenbeautel, and D. Meschede, Appl. Phys. B: Lasers Opt. **78**, 711 (2004).

[22] K. M. Birnbaum, Ph.D. thesis, California Institute of Technology, 2005.

[23] T. Wilk, S. C. Webster, H. P. Specht, G. Rempe, and A. Kuhn, Phys. Rev. Lett. **98**, 063601 (2007).

[24] A. S. Parkins, P. Marte, P. Zoller, and H. J. Kimble, Phys. Rev. Lett. **71**, 3095 (1993).

[25] T. Wilk, S. C. Webster, A. Kuhn, and G. Rempe, Science **317**, 488 (2007).

[26] Since there are two polarization degrees of freedom, the cavity modes occur in nearly degenerate pairs.

[27] R. Miller, T. E. Northup, K. M. Birnbaum, A. Boca, A. D. Boozer, and H. J. Kimble, J. Phys. B **38**, S551 (2005).

[28] J. McKeever, J. R. Buck, A. D. Boozer, A. Kuzmich, H.-C. Nägerl, D. M. Stamper-Kurn, and H. J. Kimble, Phys. Rev. Lett. **90**, 133602 (2003).

[29] A. D. Boozer, Ph.D. thesis, California Institute of Technology, 2005.

[30] A. Boca, R. Miller, K. M. Birnbaum, A. D. Boozer, J. McKeever, and H. J. Kimble, Phys. Rev. Lett. **93**, 233603 (2004).

[31] The FORT-Raman pair generates a Raman coupling between the hyperfine ground states that is proportional to $\vec{J} \cdot (\hat{\epsilon}_F \times \hat{\epsilon}_R)$, where $\vec{J}$ is the electron angular momentum operator and $\hat{\epsilon}_F$, $\hat{\epsilon}_R$ are the polarization vectors for the FORT and Raman beams, so in general $\Delta m = \pm 1, 0$ transitions are possible [29]. For our system $\hat{\epsilon}_F \times \hat{\epsilon}_R = \hat{z}$, so only the $\Delta m = 0$ transitions are driven.

[32] The FORT and Raman beams give level shifts $U_F \sim \Omega_F^2 / \Delta$ and $U_R \sim \Omega_R^2 / \Delta$, and the effective Rabi frequency for the Raman transitions driven by the FORT-Raman pair is $\Omega_E \sim \Omega_F \Omega_R / \Delta$, where $\Omega_{F,R}$ are the Rabi frequencies of the FORT and Raman beams, and Δ is the detuning from atomic resonance. Thus, the ratio of the level shifts is $U_R / U_F \sim (\Omega_E / U_F)^2 \sim 10^{-5}$ for the typical values $U_F = (2\pi)(45 \text{ MHz})$, $\Omega_E = (2\pi)(120 \text{ kHz})$.

[33] J. McKeever, J. R. Buck, A. D. Boozer, and H. J. Kimble, Phys. Rev. Lett. **93**, 143601 (2004).

[34] M. H. Anderson, R. D. Jones, J. Cooper, S. J. Smith, D. S. Elliott, H. Ritsch, and P. Zoller, Phys. Rev. Lett. **64**, 1346 (1990).

[35] K. P. Dinse, M. P. Winters, and J. L. Hall, J. Opt. Soc. Am. B **5**, 1825 (1988).

[36] S. Lathi, S. Kasapi, and Y. Yamamoto, Opt. Lett. **21**, 1600 (1996).

[37] T. Yabuzaki, T. Mitsui, and U. Tanaka, Phys. Rev. Lett. **67**, 2453 (1991).